Vision Res. Vol. 24, No. 12, pp. 1977–1990, 1984
Printed in Great Britain.

0042-6989/84 $3.00 + 0.00

SPATIAL SUMMATION IN VISUAL NOISE

DANIEL KERSTEN*
The Physiological Laboratory, University of Cambridge, Cambridge CB2 3EG, England

(*Received* 17 *August* 1983)

Abstract—Contrast thresholds were measured for sinusoidal gratings, with Gaussian spatial and temporal envelopes, as a function of spatial extent in the presence and absence of dynamic white noise. Spatial frequencies ranged from 0.5 to 32 c/deg. Efficiency is defined as the ratio of the ideal's contrast-energy threshold to that of the observer under study, each at the same performance level. For spatial frequencies from 0.5 to 8 c/deg, efficiencies for gratings in noise ranged from 8 to 30% for widths less than one cycle, but dropped rapidly as the width was increased beyond one cycle. Spatial summation of gratings in noise resembles the performance of a cross-correlator whose template is matched to a signal about 1 cycle wide (between 1/e points). The psychometric function slope is consistent with this idea.

Contrast detection Visual noise Efficiency

INTRODUCTION

In 1857 Forster found that threshold light intensity was inversely related to the size of a light spot (see Graham *et al.*, 1939). There have been numerous investigations of spatial summation since then, Ricco's and Piper's laws are well known laws put forward in the 19th century to describe spatial summation for spots against a dark field in the periphery and fovea (see Graham *et al.*, 1939). Ricco's law says that the area–intensity product is constant within some region. Piper's law says that the intensity threshold is inversely proportional to the square root of area. Subsequent studies explored the effects of background luminance and duration on spatial summation (Stiles and Crawford, 1934; Blackwell, 1946; Barlow, 1958). The applicability of these two laws varies considerably. Under photopic conditions, Ricco's law typically applies to regions of the fovea less than 1′ or so (Blackwell, 1946). Piper's law applies to rather limited regions of transition from Ricco-behavior to regions of little or no summation (Barlow, 1958).

In more recent times, spatial-frequency analysis of vision has led to the measurement of spatial summation for sine-wave gratings. There have been a number of studies of threshold spatial summation of grating patterns (Hoekstra *et al.*, 1974; Savoy and McCann, 1975; Estevez and Cavonius, 1976; Legge, 1978; Howell and Hess, 1978; Robson and Graham, 1981; Watson *et al.*, 1983). Contrast thresholds decrease with increasing width, however, beyond a certain "critical width" (about 8–10 cycles for foveal viewing), contrast thresholds decrease very little if at all (Howell and Hess, 1978; Robson and Graham, 1981). Generally, when contrast thresholds for various spatial frequencies are plotted in terms of the number of cycles, the shapes of the functions are similar.

This study investigates spatial summation at high contrasts by introducing luminance noise into the detection task. Adding a sufficient amount of visual noise raises contrast thresholds. High contrast processing can then be studied with the same methods and rigor as low contrast processing. Visual noise, whether due to the inherent stochastic nature of photon absorption or whether artificially introduced as luminance noise, presents computable limits to ideal performance. By comparing human performance to the ideal, it is possible to calculate, on an absolute scale, how well human observers combine over space, pattern information for sine-wave gratings. *Efficiency* is the measure of "how well" a pattern is detected. It is shown that to a first approximation, efficiency for detection in noise varied with width as would be expected from cross-correlation with a fixed template. Further the slope of the psychometric function was consistent with this idea.

Computation of ideal performance

In order to describe the stimuli and to compute ideal performance, several definitions are needed.† In this study, contrast varied in only one spatial dimension and time, however, the definitions are easily extended to three dimensions. The *contrast function* $c(x,t)$ is the normalized luminance minus one

*Present address: Walter S. Hunter Laboratory of Psychology, Brown University, Providence, RI 02912, U.S.A.

†The definitions are consistent with those of Pelli (1981), differing only in several qualifying adjectives, e.g. "contrast energy" vs "signal energy". Only one spatial dimension is included in the definitions here, because vertical height was not a parameter in this study. The definitions are easily generalized to include an added spatial dimension. See Watson, Barlow and Robson (1983) for an application of these definitions to quantum efficiency.

$$c(x,t) = L(x,t)/L_0 - 1$$

where $L(x,t)$ is the luminance at point x degrees (of visual angle) and at time t seconds, and L_0 is the mean luminance (Linfoot, 1964). *Contrast power* c^2, is the variance of the contrast function and is dimensionless. *Contrast energy* s^2 is the squared constrast function integrated over space and time and has dimensions of space multiplied by time (sec-deg). Appendix 1 gives an exact expression for the contrast energy of patterns used in this study. The appendix shows that contrast energy is proportional to the Michelson contrast squared, width and duration. The *noise spectral density* n^2 of one-dimensional dynamic noise, is the contrast power of luminance noise in a 1 c/deg by 1 Hz band and has units of sec-deg. *White noise* has constant noise spectral density. When a pattern to be detected is known exactly, and is to be detected against a background of white Gaussian noise, the ideal's performance is determined by the ratio of the contrast energy to the noise spectral density. The square root of this ratio, called the *signal-to-noise* ratio, is equal to $\sqrt{2}$ times the normal deviate (Z) of the ideal's proportion correct in a two-alternative forced-choice (2AFC) task

$$\sqrt{2}Z = d' = s_i/n_i$$

where s_i^2 and n_i^2 are the contrast energy and noise spectral density. This result is a straight forward extension to two dimensions of one given by Green and Swets (1974) for one dimension.

There are several ways of defining efficiency. The first one, due to Tanner and Birdsall (1958) is more general and is useful for computation but is rather opaque at first reading. The second is more restrictive, but intuitively easier to grasp. The *efficiency* E, for detection is defined as the square of the ideal's signal-to-noise ratio divided by the signal-to-noise ratio required by the human, each at the same performance level

$$E = (s_i/n_i)^2/(s_0/n_0)^2$$

where the denominator, $(s_0/n_0)^2$ is the square of the threshold signal-to-noise-ratio of the observer. The "performance level", in the current study, refers to the proportion correct in a two-alternative forced-choice detection task.

The second, rather simpler way of thinking about efficiency, is as follows. Imagine that the contrast threshold of the ideal observer is measured under the same conditions and for the same signal as the human observer, and a contrast threshold of c_i is found. If the contrast threshold of the human observer is c_0, then the efficiency is the squared ratio of the ideal's contrast threshold to the human's

$$E = (c_i/c_0)^2.$$

This equation derives from the previous one when

$$n_i = n_0 \text{ and when } s_i \propto c_i \text{ and } s_0 \propto c_0.$$

Human detection performance resembles that of the ideal and is said to be "ideal-like" when efficiency is constant as a function of the parameter of interest. When human spatial summation is ideal-like over a certain range of widths *ideal summation* is said to occur. Ideal summation occurs when contrast-energy thresholds are constant as a function of width or equivalently when contrast thresholds are inversely proportional to the square root of width. No summation is said to occur when contrast thresholds are constant as a function of width. To describe a region of spatial integration as ideal summation says nothing about how good performance is, but only how thresholds change with width.

METHOD

Apparatus

The signal patterns were vertical sine-wave gratings with Gaussian horizontal spatial and temporal windows. Gaussian enveloped cosine and sine waves will be referred to as Gabor functions (Gabor, 1946). The patterns were produced on the face of a Joyce Electronics CRT display by Z-axis modulation (Campbell and Green, 1965). The display was of the electromagnetic deflection type, with a raster frequency of 100 kHz, and a noninterlaced frame rate of 100 Hz. The display had a P31 phosphor, an unmodulated luminance of 340 cd/m^2, and a dark surround. In order to achieve a wide range of spatial frequencies and windows, viewing distances of 57, 228, 456 and 912 cm were used. Unless otherwise mentioned, all data for a given spatial frequency were collected at the same viewing distance. The display was 30 cm wide and 16 cm high. Thus, at the viewing distance of 228 cm, the screen subtended 7.5° horizontally by 4° vertically. Photometric calibrations were conducted with an UDT 80X Opto-meter, which was photopic-luminance corrected.

The signal-luminance waveforms were synthesized digitally by an LSI-11/23 computer. In each 10 msec frame, the computer generated 300 pairs of voltage samples which were routed through two 12-bit digital-to-analog converters (DAC). One DAC generated the spatial envelope, and the other the sinusoidal grating. The outputs of the two DACs were then multiplied and routed through a programmable dB attenuator which temporally modulated the signal voltage which was subsequently added to the noise.

The luminance noise varied in time and in the horizontal spatial dimension. Pseudorandom noise was digitally synthesized by a 31-bit shift register with exclusive-or feedback (Roberts, 1963; Horowitz and Hill, 1980; Pelli, 1981). To produce Gaussian one-dimensional noise, the shift register was clocked at f_c and low-pass filtered at a corner frequency of $0.1 \times f_c$. This is analagous to the familiar construction of a Gaussian random variable by addition of several uniformly distributed random variables. The spatial frequency bandwidth of the noise was always kept flat to at least 3 c
frequency. The temporal
100 Hz. At the maximum
noise generator would cyc
6 hr.

Procedure

Contrast thresholds were
width, by a two-alternative
while keeping the spatial
constant. Contrast thresh
maximum of the contrast
threshold. A maximum-l
used to present the sign
estimate of threshold cor
1983). Unless otherwise in
ing 75% correct was estima
of 4 blocks of 40 trials ea
threshold.

Models of contrast det
count the psychometric fur
functions were measured ir
of visual noise. A two-alte
cedure was used. In keepir
mental strategy of trying t
certainty regarding the sig
cent correct was measured
contrast. There were five b
session. All psychometric
on data lumped from at
minimum of 1000 trials.

To reduce stimulus unce
sample of the signal was
each trial. For the visual n
signal was shown in the ab
noise conditions, the sign
increase in the dB level o
intervals were separated b
was marked by an audito
indicated to the observer
noise was turned on abru
peak contrast was reached
160 msec after the peak c
time-constant of the Gauss
extended uniformly across
gular spatial and tempora

Observers

There were two observer
was naive to the details of
and D.R. are emmetropi
with natural pupils, and
(2 mm dia) at the center c

RESU

Contrast thresholds

For clarity, but at the ex
the data are presented i

kept flat to at least 3 octaves above the signal frequency. The temporal frequency bandwidth was 100 Hz. At the maximum rate used (200 kHz), the noise generator would cycle once ($2^{31} - 1$ shifts) in 6 hr.

Procedure

Contrast thresholds were measured as a function of width, by a two-alternative forced-choice procedure, while keeping the spatial and temporal frequencies constant. Contrast threshold was defined to be the maximum of the contrast function of the pattern at threshold. A maximum-likelihood procedure was used to present the signal at the current "best" estimate of threshold contrast (Watson and Pelli, 1983). Unless otherwise indicated, the contrast yielding 75% correct was estimated. Typically, a minimum of 4 blocks of 40 trials each were used to determine threshold.

Models of contrast detection must take into account the psychometric function. Thus, psychometric functions were measured in the presence and absence of visual noise. A two-alternative forced-choice procedure was used. In keeping with the general experimental strategy of trying to maximize the observer's certainty regarding the signal to be detected, the per cent correct was measured in 100 trial blocks for each contrast. There were five blocks at five contrasts per session. All psychometric function slopes are based on data lumped from at least two sessions and a minimum of 1000 trials.

To reduce stimulus uncertainty, in all conditions, a sample of the signal was shown 600 msec prior to each trial. For the visual noise conditions, the sample signal was shown in the absence of noise. For the no noise conditions, the signal was shown at a 30% increase in the dB level of the signal contrast. The intervals were separated by 600 msec. Each interval was marked by an auditory tone. A feedback tone indicated to the observer whether he was right. The noise was turned on abruptly 160 msec before the peak contrast was reached, and turned off abruptly 160 msec after the peak contrast was reached. The time-constant of the Gaussian was 80 msec. The noise extended uniformly across the screen and had rectangular spatial and temporal envelopes.

Observers

There were two observers. D.K. is the author. D.R. was naive to the details of the experiment. Both D.K. and D.R. are emmetropic. Viewing was binocular with natural pupils, and with a black fixation disk (2 mm dia) at the center of the pattern.

RESULTS

Contrast thresholds

For clarity, but at the expense of some redundancy, the data are presented in terms of contrast and contrast-energy thresholds. Figure 1(a) and (b) show data for observers D.K. and D.R. respectively. Contrast thresholds are plotted as a function of width for 0.5, 2, 8 and 32 c/deg gratings in separate panels for each subject. Data collected in high noise are shown in the upper set of points for each graph.

Regions of ideal and no summation are illustrated for the 8 c/deg data of Fig. 1(b) (top right panel) by the solid lines which were fit to the data by eye. For the lower, no noise data, as width increases, thresholds continue to decline out to at least 4–8 cycles. The slope is about -1 for small widths and approaches 0 for larger widths. On the other hand, contrast thresholds for gratings in noise, the upper points, drop rapidly only out to about a cycle, after which they are constant or increase somewhat. Ideal summation is shown on the graph by a line of slope of -0.5, and no summation by a line of slope 0. Probability summation slopes generally fall between these two (Robson and Graham, 1981). A typical slope (for the no noise condition) of about -0.3 is shown by the dashed line (see Discussion). The data for 0.5 and 2 c/deg follow a similar trend. However, the data for the 32 c/deg gratings do not follow this pattern. In the absence of noise, contrast thresholds at 32 c/deg actually rise from 0.25 to 2 cycles, whereas over the same region, thresholds in noise either remain fairly constant or drop slightly.

Contrast energy thresholds

Because efficiency is inversely proportional to contrast-energy threshold, it is informative to plot contrast-energy thresholds as a function of width. Figure 2(a) and (b) show the data from Fig. 1(a) and (b) replotted in terms of contrast-energy thresholds in sec-deg. In these coordinates, ideal summation falls along lines of slope 0, and no summation along lines of slope $+1$. The upper right panel of Fig. 2(b) illustrates these two regions of summation by the solid lines which were fit by the eye. The dashed lines, described below, are the results of a bi-linear fit to the noise data. Except for the 32 c/deg data, contrast–energy thresholds in the absence of noise do not rise as rapidly as in the presence of noise. For the 8 c/deg data, the contrast–energy thresholds fall for narrow gratings until about 1 cycle. In high noise, for 0.5, 2 and 8 c/deg, a dramatic rise in contrast–energy threshold begins at about one cycle. There is evidence for a decline in contrast–energy threshold (discussed below) from very narrow widths to the critical width. The computed slopes are discussed below.

In contrast to the other spatial frequencies, the contrast-energy thresholds for the 32 c/deg data rise from the very narrowest width (0.0079°) both in noise and in the absence of noise, which corresponds to a quarter of a cycle. There was no summation in noise for the 32 c/deg grating from 0.25 to 4 cycles for D.K. and from 0.25 to 2 cycles for D.R. in the absence of noise.

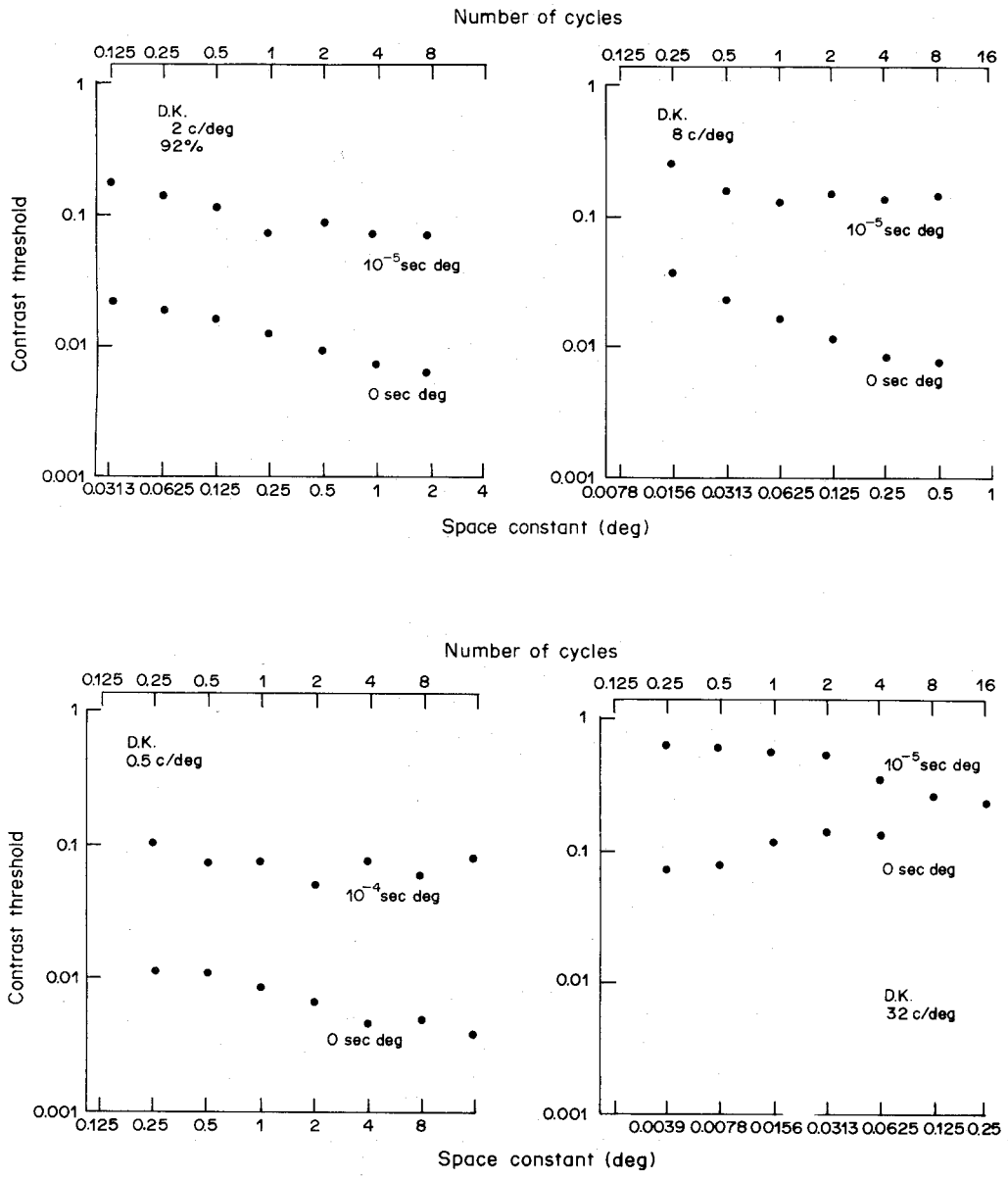

Fig. 1(a)

Efficiency

In Fig. 3(a) and (b) efficiency is plotted as a function of the number of cycles for detection of gratings of 0.5, 2, 8 and 32 c/deg in noise.* These efficiencies were all computed from the data presented in Fig. 2.

The efficiency is quite high for gratings less than a cycle wide, 20–40% for the 0.5 and 2 c/deg data, size varied and with it the eye's state of adaptation. The role of vertical height in the detection of vertical gratings has been discussed by Howell and Hess (1978) and Wright (1982). In addition to various viewing distances, the 2 c/deg data for D.K. was taken from a different point of the psychometric function (92%) and the 5 c/deg data was collected at a different noise level ($n^2 = 10^{-4}$ sec deg). Because the psychometric function slope is close to one for detection in noise (see Table 2 and below), and contrast–energy thresholds are linearly related to noise spectral densities (Pelli, 1981), the differences in conditions lead to rather small differences in efficiency. However, any departures from these linearities could account for higher (or lower) efficiencies for 0.5 and 2 c/deg for D.K.'s data as compared with D.R.'s. The important point is that the efficiencies remain rather high (above 8%) for widths of 0.25 to 1 cycle regardless of spatial frequency in the range 0.5–8 c/deg.

*Comparison of efficiency between various spatial frequencies has to be done with some care. The data for D.R. were all collected under identical conditions expect that the viewing distance, and thus the angular screen size was different for the various conditions: 57 cm for the 0.5 c/deg grating 228 cm for the 2 c/deg grating and 912 cm for the 8 and 32 c/deg gratings. Thus the vertical

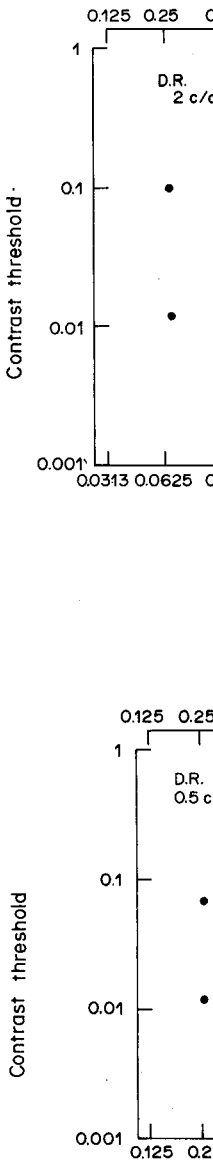

Fig. 1.(a) Contrast
terms of the space
between 1/e points
the presence and al
10^{-5} sec-deg for all
thresholds at the 92
thresholds were me
more thresholds. E
minus one and a ha
upper left, upper ri
for Fig. 1(a). In ac
fit by eye). The da
summation a

10–15% for the 8 c/deg
32 c/deg grating for D.
noise varied in only o
impossible to strictly com

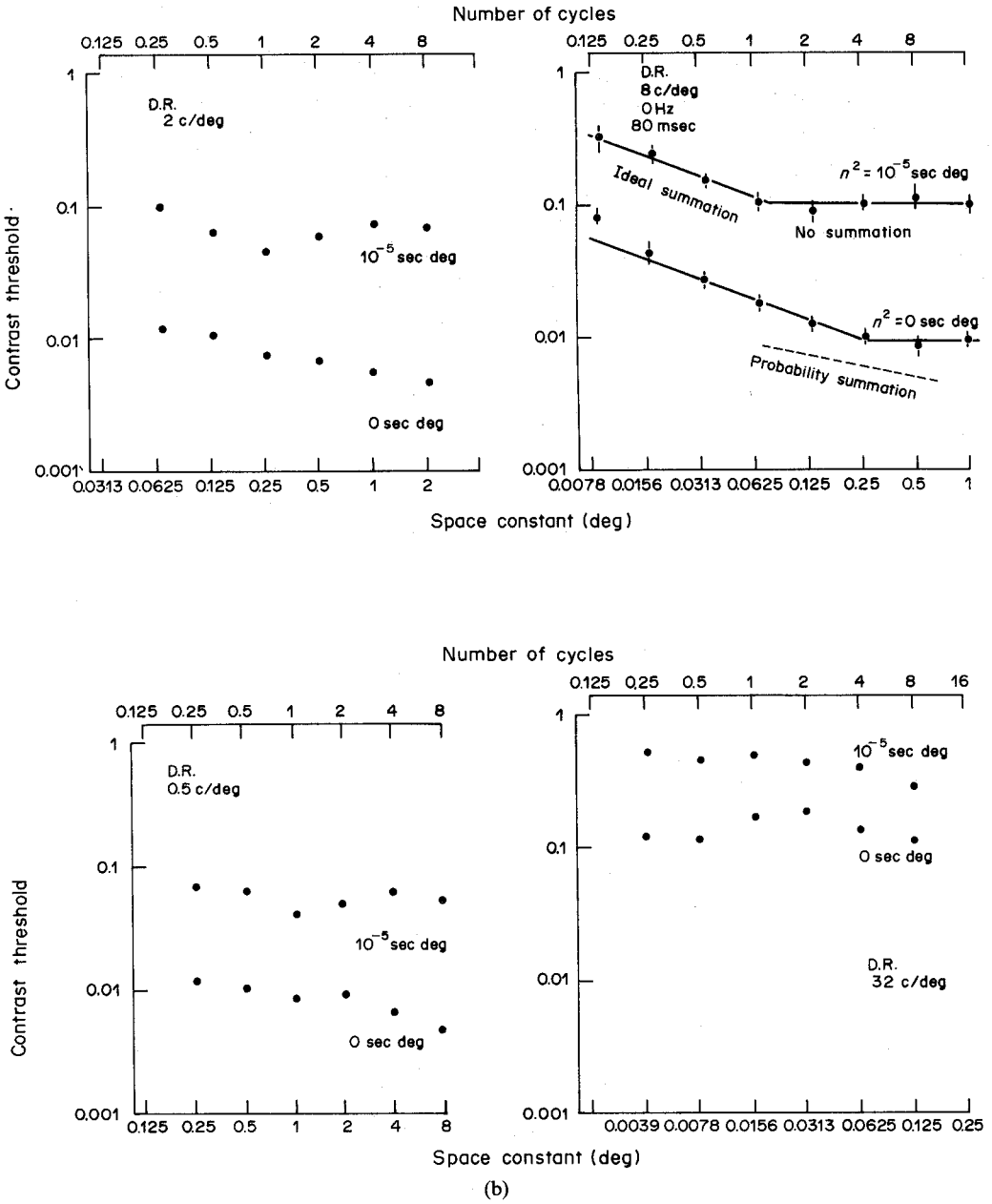

(b)

Fig. 1.(a) Contrast thresholds as a function of width. In each panel, the lower abscissa shows width in terms of the space constant of a Gaussian window and the upper abscissa shows the number of cycles between 1/e points. The upper and lower sets of points in each panel represent thresholds measured in the presence and absence of one dimensional dynamic noise, respectively. The noise spectral density was 10^{-5} sec-deg for all but the 0.5 c/deg data where it was 10^{-4} sec-deg. The 2 c/deg data represent contrast thresholds at the 92% correct point. These data were collected at a viewing distance of 456 cm. All other thresholds were measured at the 75% correct point. Each point represents the geometric mean of four or more thresholds. Except for one point, the standard errors are less than 15%, corresponding to plus or minus one and a half symbols width. The spatial frequencies are 0.5, 2, 8 and 32 c/deg for the lower left, upper left, upper right and lower right panels respectively. Observer D.K. (b) Observer D.R. Details as for Fig. 1(a). In addition, the upper right panel shows regions of ideal and no summation (solid lines, fit by eye). The dashed line shows the slope predicted from a probability summation model of spatial summation assuming a psychometric function slope of 3.3 as is often found without noise.

10–15% for the 8 c/deg data and 3–6% for the 32 c/deg grating for D.K. Because the luminance noise varied in only one spatial dimension, it is impossible to strictly compare efficiencies for the data collected in the absence of noise with the data of Fig. 3. However, it can be noted that the highest efficiencies reported for stimuli detected against a uniform field (340 cd/m^2) are usually less than 0.05%

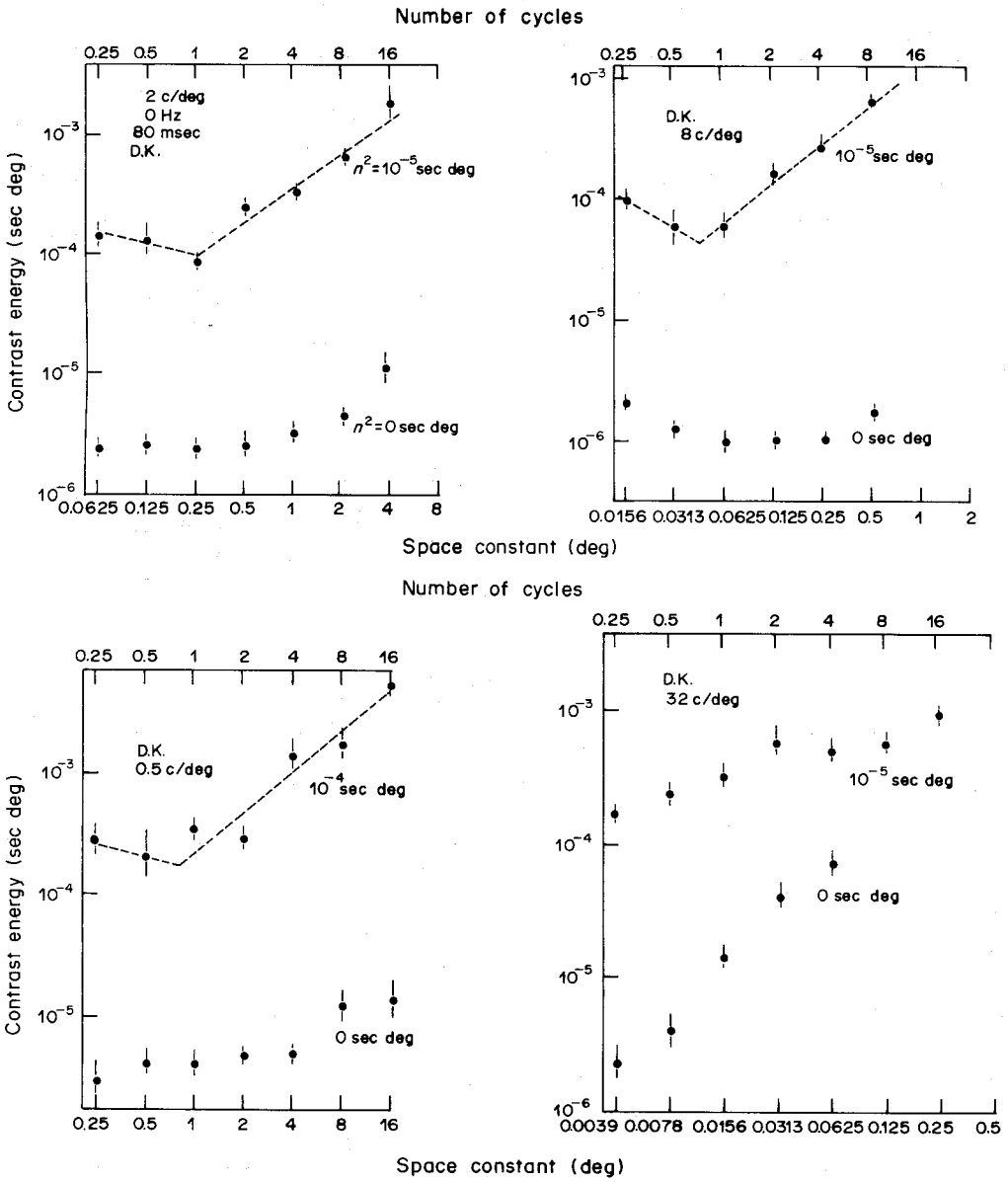

Fig. 2(a)

(Watson *et al.* 1983). As was noted in the contrast energy plots, the efficiency is high for gratings less than a cycle or so in width, but drops sharply, with slopes close to -1, for widths much more than a cycle or 2. Evidence is provided below suggesting a local maximum in efficiency for one cycle's width. Again note that the 32 c/deg data do not fit well into this otherwise uniform picture. Efficiency is highest for very narrow bars, about 30″ wide (0.25 cycles between 1/e points), and drops fairly rapidly, but not as rapidly as for the lower frequency gratings, the slope being about -0.4 over the range from 0.25 to 16 cycles.

Bi-linear regression fits

In order to quantify the above observations concerning critical width, a bi-linear regression fit was made to the data of Fig. 2. This procedure was developed by Hinkley (1969; 1971) to find the maximum likelihood intersection for a two-limbed linear regression fit. The data were fit for numbers of cycles greater than 0.25 and for spatial frequencies 0.5, 2, and 8 c/deg. Table 1 shows the critical width, the "lower" slopes ($k1$) of contrast–energy thresholds over widths less than the critical width and "upper" slopes ($k2$) over widths greater than the critical width. It can be seen that for all cases, the critical width is near one. The mean value is 0.86. The slopes over points less than the critical width and greater than the critical width have a means of -0.39 and 1.10. For all cases the slope over widths less than the critical width is less steep than over widths greater

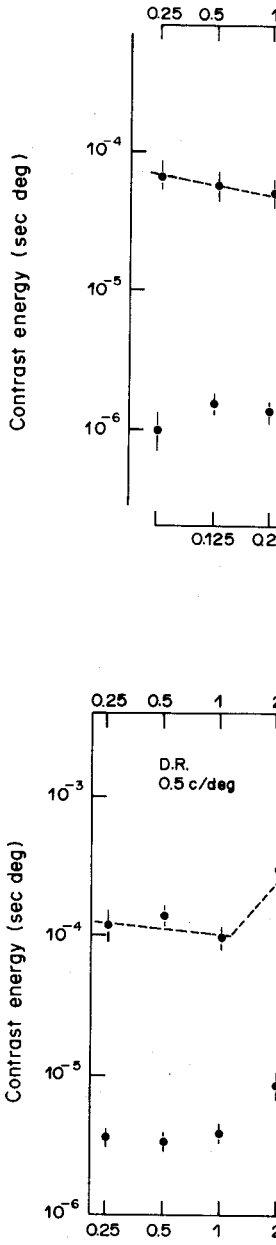

Fig. 2.(a) Data from
Fig. 1. The dashed lin
(b) Data from Fig. 1(
Fig. 2(a). In addition,

than the critical width.
regression fits were made o
greater for the no noise c
column in Table 1). 95% c
computed on the slopes. In
data collected in the a
significantly less than slope

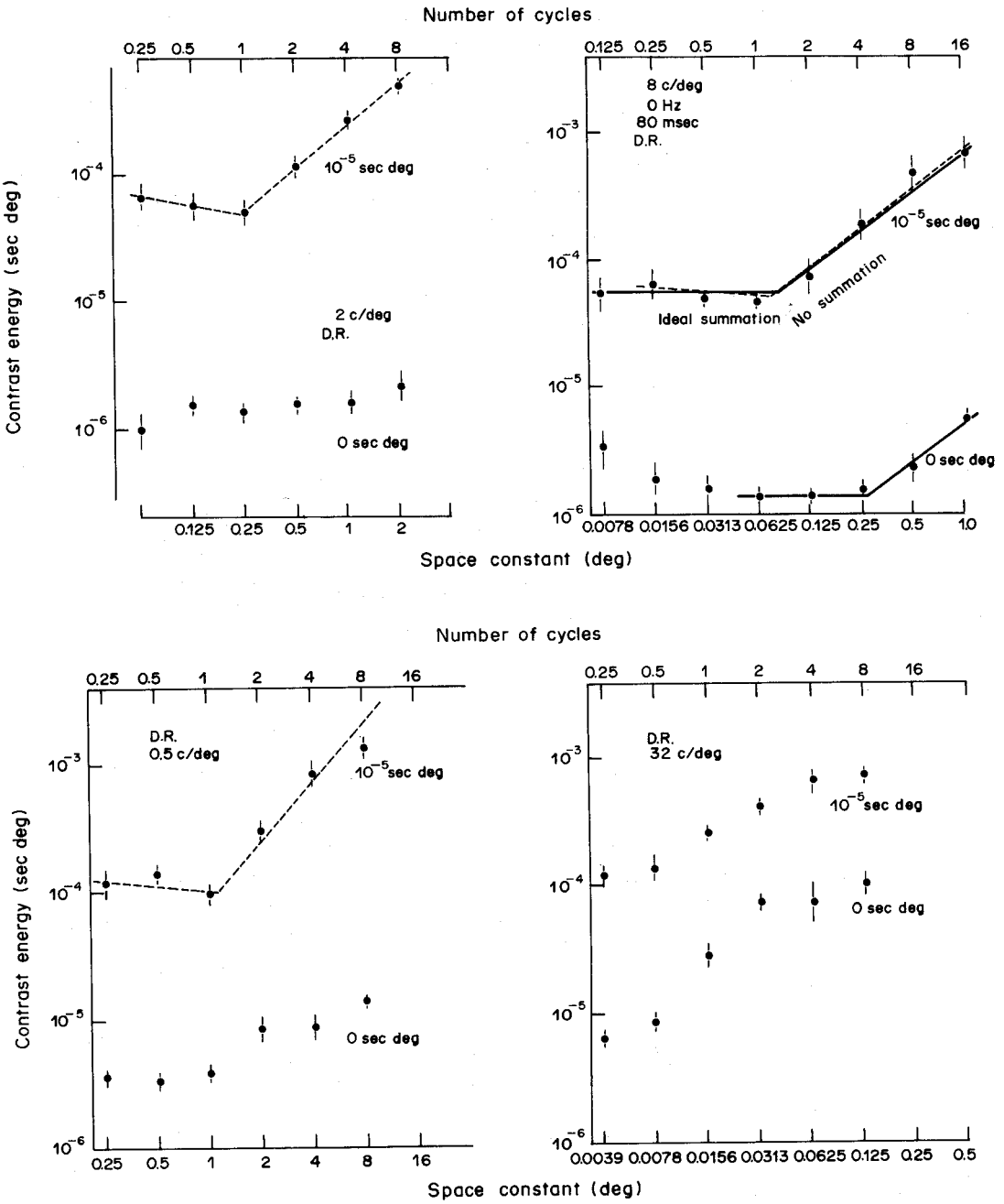

(b)

Fig. 2.(a) Data from Fig. 1(a) replotted as contrast–energy thresholds vs width. The abscissas are as for Fig. 1. The dashed lines represent bi-linear fits to the data over a range of 0.25–16 cycles. Observer D.K. (b) Data from Fig. 1(b) replotted as contrast-energy thresholds vs. width. Observer D.R. Details as for Fig. 2(a). In addition, the upper right panel shows solid lines (fit by eye) which illustrate regions of ideal and no summation.

than the critical width. For comparison, linear regression fits were made over widths with a cycle or greater for the no noise condition (see right-most column in Table 1). 95% confidence intervals were computed on the slopes. In all cases, the slopes for data collected in the absence of noise were significantly less than slopes for corresponding data collected in the presence of noise ($P > 0.05$). The mean slope was 0.31. The slopes for the condition labelled "cross-correlator" in Table 1 are discussed below.

Psychometric functions

The Discussion shows that to a first approxi-

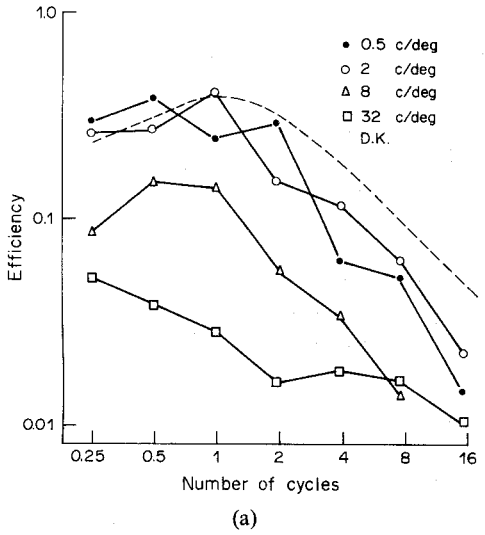

(a)

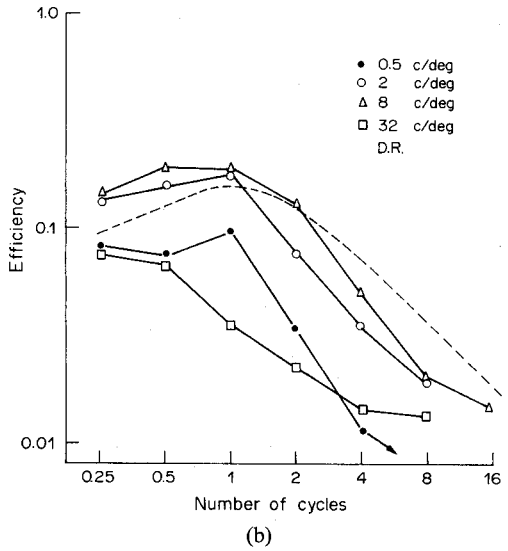

(b)

Fig. 3.(a) The thresholds measured in noise [Figs 1(a) and 2(a)] are replotted in terms of efficiency as a function of the number of cycles between 1/e points. The dashed line shows the performance of a cross-correlator (with additive noise) which is matched to the frequency and phase of the grating to be detected, but only to a width of one cycle between 1/e points. Observer D.K. (b) Observer D.R. Other details as for Fig. 3(a).

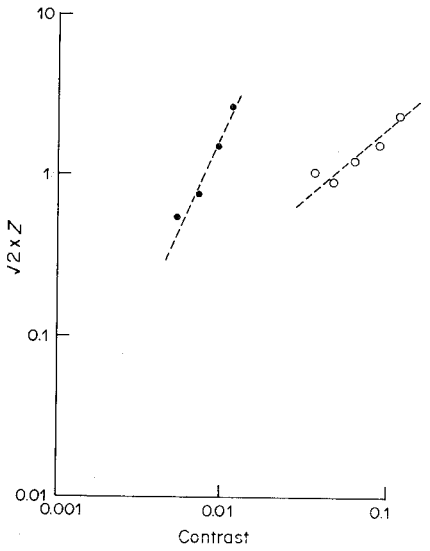

Fig. 4. Psychometric functions. Log $\sqrt{2}Z$ vs log contrast. Z is the normal deviate of the proportion correct in a 2AFC procedure. The signal was a 2 c/deg grating one cycle wide between 1/e points. It was detected in the presence (open circles) or absence (solid circles) of noise. The slope in the presence of noise (0.9) is shallower than in the absence of noise (2.3). Observer D.K.

mation, the thresholds in noise can be modeled by a cross-correlator. One property of a cross-correlator is that the normal deviate of the proportion correct is proportional to contrast. Figure 4 shows psychometric function data for D.K. for a 2 c/deg ($s_x = 0.25°$) grating in the presence and absence of noise. (This pattern was detected with the highest efficiency in noise. Other conditions are summarized in Table 2.) The dependent variable of interest is the steepness, k of the psychometric function. When $\sqrt{2}$ times the Z-score of the proportion correct (Z) is plotted against contrast (c) on log–log coordinates, k represents the slope

$$\sqrt{2Z} = c^k \times \text{constant}.$$

The slope for the data collected in the presence of noise is shallower ($k = 0.85$) than the slope for the data in the absence of noise ($k = 2.28$).

Table 1. Bi-linear regression fit–log contrast energy vs log width

Subject	Spatial frequency (c/deg)	Lower slope ($k1$) (in noise)	Upper slope ($k2$) (in noise)	Critical width (cycles)	Slope from 1 to 8 cycles (in absence of noise)*
D.K.	0.5	−0.38	1.1	0.78	0.48 ± 0.24
D.K.	2	−0.37	0.92	0.88	0.20 ± 0.12
D.K.	8	−0.8	1.1	0.69	0.23 ± 0.18
D.R.	0.5	−0.16	1.4	1.00	0.38 ± 0.35
D.R.	2	−0.24	1.1	0.92	0.21 ± 0.26
D.R.	8	−0.40	1.0	0.88	0.47 ± 0.20
		Mean = −0.39	1.10	0.86	0.31
Cross-Correlator		−0.39	0.9	1.4	—

*The ± signs indicate 95% confidence intervals.

Table 2. Psychometric function data

Subject	Spatial frequency (c/deg)	Width (deg)	Noise spectral density (sec deg)	Number of trials	Slope* (k)
D.K.	2	0.25	10^{-5}	1000	0.85 (0.61–1.19)
D.K.	2	0.25	0	1200	2.28 (1.63–3.19)
D.K.	0.5	1.00	10^{-5}	1200	1.15 (0.82–1.61)
D.K.	0.5	1.00	0	1300	2.34 (1.67–3.28)
D.R.	2	0.25	10^{-5}	1200	1.04 (0.74–1.46)
D.R.	2	0.25	10^{-5}†	1250	1.37 (0.98–1.92)
D.R.	2	0.25	0	1200	2.86 (2.04–4.00)
D.K.	32	0.0156	10^{-5}	1500	2.67 (1.91–3.74)
D.R.	32	0.0156	10^{-5}	1350	2.62 (1.87–3.67)

*The numbers in parentheses represent 95% confidence intervals for the slopes.
†These data were collected in continuous noise.

Psychometric function data for several other conditions are summarized in Table 2. Three spatial frequencies are represented, 0.5 and 2 c/deg in the presence and absence of noise and 32 c/deg only for the noise condition. The widths were all one cycle between 1/e points. The slopes were computed using a maximum likelihood procedure originally developed by Watson (1979) and modified by Rubin (1982) to fit a Gaussian distribution. The 95% confidence intervals indicated in parentheses were estimated by Monte Carlo simulations assuming binomial statistics. 1000 stimulations of psychometric functions were run for values of $k = 1$, 2 and 3. The proportions correct were 0.55, 0.65, 0.75, 0.85 and 0.95. The slopes were approximately lognormally distributed. The estimated 95% confidence intervals for $k = 1$, 2, and 3 were approximately equal: ± 0.14, ± 0.15 and ± 0.15 log units respectively. The criterion corresponding to ± 0.15 was adopted for all conditions. By this criterion, slopes for 0.5 and 2 c/deg in noise are not significantly different from one.

DISCUSSION

Thresholds in noise—models

There are several explanations of the spatial summation of gratings in noise which should be considered. The first is a detector which only looks at the peak of the contrast function of the signal. In fact, observers do report that if they want "to do their best", they try to ignore all but the central region of the pattern. But such a model predicts that efficiency should drop with a slope of -1 (in Fig. 3) from the narrowest to the broadest width regardless of spatial frequency. Efficiency does drop with a slope of about -1, but only for widths greater than a cycle or so.

A second explanation is in terms of spatial probability summation among independent detectors. Probability summation has been used with good success to describe spatial summation of gratings in the absence of noise by Legge (1978) and Robson and Graham (1981). For the moment assume homogeneity in sensitivity across the visual field. According to Robson and Graham, contrast threshold, c is proportional to $n^{-1/p}$, where p is a measure of psychometric function steepness based on the Quick function and n is the number of cycles. The measure of steepness (k) used in Table 2 is equal to $0.83 \times p$ (Pelli, 1981). In terms of contrast energy (s^2), probability summation predicts s^2 is proportional to $n^{(-0.83\times 2)/k+1}$. The average slope from Table 2 is 1.12. Thus, contrast energy should be proportional to $n^{-0.48}$. Only one of the negative slopes in Table 1 is this steep (i.e. -0.48), and for regions greater than the critical width, the slopes are all near 1. Watson (1982) estimated 3/8 dB (about 0.02 log units) drop in sensitivity per period from the data of Robson and Graham (1981) for thresholds of grating patches for increasing eccentricity in the absence of noise. This is too small to account for the fact that there is virtually no summation beyond the critical width. Of course, there remains the possibility that there is an unusual reduction in sensitivity for gratings in noise away from the fovea. This has not been checked.

A third model to consider is the energy detector (Green and Swets, 1974). This model predicts that contrast–energy thresholds should be constant as a function of width. This is clearly not the case. However, regions of approximate ideal summation do exist. The energy detector predicts psychometric function slopes (k), in noise, equal to 2. This is too high.

The fact that the psychometric function slope is near one, suggests that a cross-correlator (to be described shortly) might fit the data of Fig. 3. Burgess *et al.* (1981) have argued that for discrimination of certain gratings in static noise, efficiencies are high enough to rule out most models except for a cross-correlator. Although the efficiencies reported here are not high enough to rule out incoherent detection or multiple channel models, the performance of a cross-correlator tuned to a Gaussian-enveloped sinusoid one cycle wide between 1/e points* provides a good first order approximation to the data. One cycle's

*_Coherent detection_ refers to detection when phase information is used, and _incoherent detection_ refers to detection when phase is not used in the detection algorithm. Cross-correlation is example of coherent detection. Envelope and energy detectors are examples of incoherent detectors. No incoherent detector can match the performance of the best coherent detector, when phase information is in principle available.

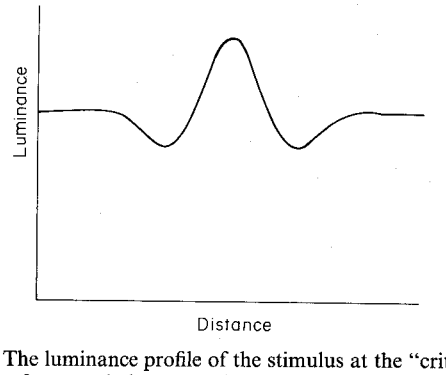

Fig. 5. The luminance profile of the stimulus at the "critical width" of one cycle between 1/e points. A local maximum in efficiency was found for stimuli of this shape (i.e. with respect to variation in width) from 0.5 to 8 c/deg. The profile represents a cosine function one cycle wide between 1/e points of a Gaussian window.

width is chosen because this is where a local maximum in efficiency seems to occur.

The cross-correlator is a realization of the ideal detector when the signal is known exactly (Green and Swets, 1974). If the filter has a fixed space constant, phase and spatial frequency, then it is optimal only for that space constant, phase and spatial frequency and is "mis-matched" for the other widths, phases and spatial frequencies. Suppose that the detector is tuned to the center spatial frequency of the stimulus but is matched to only one width, i.e. one cycle wide. This means that the bandwidth is a fixed number of octaves (2.2 octaves between 1/e points or 1.7 octaves at half height).*

Let $f(x)$ represent the filter

$$f(x) = \exp\{-(x/s_0)^2\}\cos 2\pi f x$$

where s_0 is the space constant, f the spatial frequency and x the distance in degrees of visual angle. Both f and s_0 are assumed to be fixed while the detector looks at gratings of frequency f, but various widths s_x. Let $c(x)$ be the contrast function for the signal

$$c(x) = c_m \exp\{-(x/s_x)^2\}\cos 2\pi f x$$

where c_m is the Michelson contrast prior to windowing. Then the response output, r_0, of the cross-correlator is given by the cross-correlation of the filter with the observation $c(x) + n(x)$

$$r_0 = \int f(x)\{c(x) + n(x)\}\mathrm{d}x$$

when the signal is present, and with the observation $n(x)$

$$r_0 = \int f(x)n(x)\mathrm{d}x$$

when the signal is absent. $n(x)$ is the contrast function of the noise sample. Because r_0 is monotonic with likelihood ratio, and because the variance of r_0 is independent of the signal parameters, the mean of r_0 determines the error rate in a two-alternative forced-choice experiment. Appendix 2 derives the performance of the cross-correlator in detail.

The dashed lines in Fig. 3(a) and (b) represent the performance of a cross-correlator tuned to the spatial frequency of interest and with a bandwidth between 1/e points of 2.2 octaves. The dashed line describes how the efficiency of this filter varies with the number of cycles of the signal. The actual efficiency is 1 at one cycle. However, by assuming additive intrinsic noise, the vertical height of the line can be varied. The significance of the lack of agreement in absolute efficiency at one cycle is considered below. The results of a bi-linear fit to this cross-correlator's log contrast energies as a function of log width are shown in Table 1. The critical width is 1.4. The slopes for widths less than and greater than the critical width are -0.39 and 0.90 respectively. These slopes are not significantly different from the mean of -0.39 and 1.1 of the human data. However, as considered below, the lower slope is shallower than the cross-correlator's when very narrow widths are included in the fit for at least two conditions.

Although the cross-correlator model accounts for the fall-off in efficiency reasonably well, there are several inadequacies to consider. In order to account for the fact that the efficiencies in the data are not one at one cycle, we would have to assume an equivalent additive noise of about 2–4 times that of the external noise. Using the method of Pelli (1981), the observer's "equivalent noise" is estimated by

$$n^2 s^2{}_0/s_1^2$$

where s_0^2 and s_1^2 are the contrast-energy thresholds for the no noise and noise conditions respectively (see also Burgess *et al.*, 1981). For the 2 c/deg grating with space constant 0.25° of D.K., the equivalent noise estimate is less than 3% of the noise ($n^2 = 10^{-5}$) which is only a small fraction of the equivalent noise required to account for the efficiency measured. The alternative explanation for the efficiencies being less than one is to presume that the stimuli do not match the internal templates available. This suggests that other spatial and temporal parameters could be found which would lead to higher efficiencies.

The high efficiencies found for gratings less than a cycle wide actually rule out a large class of multiple-channel models. Pelli (1984) has attempted to account for detection of gratings in the absence of noise by a "channel-uncertainty" model. This is the optimal detector for detecting one of M orthogonal signals. Nolte and Jaarsma (1967) have shown that this ideal is closely approximated by M orthogonal cross-correlators for which the decision is based on the

*This follows from the fact that the spread between 1/e points in the spatial frequency spectrum of a Gabor function is $2/(\pi s_x)$ c/deg, and that the Fourier transform of a Gabor function is a Gaussian in the frequency domain. The bandwidth at half-height in octaves is given by

$$\log_2\{(\pi n + 2\sqrt{\ln 2})/(\pi n - 2\sqrt{\ln 2})\}$$

where n is the number of cycles between 1/e points.

peak response among the M detectors. Pelli has plotted the psychometric functions as d' vs signal-to-noise ratio for various M on log–log coordinates. The case $M = 1$ corresponds to the model proposed in the current study. As M increases, the psychometric function slope (k) increases and so does the signal-to-noise ratio required to achieve a criterion proportion correct. In fact, by the time $M = 10$, the required signal-to-noise ratio to achieve $d' = 1$ has doubled. This means that a detector designed to be best at detecting one of 10 orthogonal signals has an efficiency relative to the $M = 1$ detector of 1/4 or 25%. Thus models involving combination of more than 10 orthogonal filter outputs are ruled out for the gratings in Fig. 3 which have an efficiency higher than 25%. For M greater than one, a one-of-M-orthogonal signals model would predict higher slopes than one for the psychometric functions. The slopes of the ideals, however rise gradually with M and are still within the confidence intervals of the psychometric function slopes reported here when $M = 10$. Thus a modest amount of uncertainty might improve on a single channel model with respect to both the slope and the efficiencies less than one.

The bandwidth of 1.7 octaves is similar to that found by others. Legge and Foley (1980) report 1.75 octave tuning curves for high contrast masking tuning functions. Blakemore and Campbell (1969) find broad band selective spatial frequency adaptation. Stromeyer and Julesz (1972) also found broad tuning functions using noise masks. The four mechanisms of Wilson and Bergen (1979) have bandwidths of about 1.75 octaves.

Van Meeteren and Barlow (1981) measured efficiency for the detection of static dot gratings in dot noise as a function of width of the grating. They found that efficiencies remained uniformly high (up to 50%) from 1 to 5 cycles over a wide range of spatial frequencies before dropping. High efficiency at 5 cycles corresponds to very narrow bandwidth filters (about 0.31 octaves at half height). Burgess *et al.* (1981) found efficiencies as high as 70% for contrast discrimination of Gabor functions ($f = 4.6$ c/deg, 0.55 octaves) in static noise. In the static noise experiments, the subject often is allowed unlimited viewing time and can scan the screen before making a judgment. This is in contrast to the present study, where fixation was maintained and the presentation time was short.

Physiological implications

It is possible to make some reasonable speculations about the neuro-physiological substrate for the performance found. One can conjecture that because the observer may have a poorer memory for arbitrary patterns or poorer ability to cross-correlate them, it is optimal for the observer to make use of pre-existing "hard-wired" cross-correlators.

It has been suggested that simple cell receptive fields of striate cortex have filter shapes close to that of Gabor functions (Marcelja, 1980; Sakitt and Barlow, 1982). Gabor functions have the property that they are maximally localized in space and frequency (Gabor, 1946). It can be argued that if the visual system needs to extract spatial frequency information for processing of object size and for scene analysis at different levels of detail (Marr, 1982) or for the extraction of shape from shading (Pentland, 1982), but nevertheless needs to keep track of where things are, that filters which efficiently encode both would exist.

The X-cells of the cat retina and lateral geniculate nucleus do have fairly broad bandwidths, usually greater than two octaves. However, there is evidence that retinal X-cells, in the cat, may not have the required range of center frequencies implied by the results found here (Peichl and Wassle, 1979). The simple cells of the striate cortex might provide the neuro-physiological substrate for coherent detection of stationary patterns used in this study. They are phase-selective (Movshon *et al.*, 1978; De Valois *et al.*, 1982). Further, the presence of visual noise might in fact improve the simple cell's correlation efficiency by linearizing the cell (Maffei *et al.*, 1979). Simple cells also have shallow psychometric functions as compared to human psychometric functions for gratings in the absence of noise (Tolhurst *et al.*, 1983). The bandwidths of simple cortical cells are similar to those estimated from efficiencies for signals used in this study. De Valois *et al.*, (1982) report a median simple cell bandwidth of 1.4 octaves in the macaque. However the spread is quite large, ranging from 0.4 to over 2.6 octaves.

There is at least one argument against a cortical simple cell substrate. Tolhurst and Thompson (1981) found that simple cells in the cat tend to have narrower tuning curves (on log coordinates) as the center spatial frequency increases. In fact, it can be inferred from their data that bandwidth on linear coordinates should be approximately proportional to the square root of the optimal frequency. The bandwidths, in c/deg, inferred in the current study increase linearly with optimal spatial frequency.

A physiological interpretation would suggest that there may not be phase sensitive receptive field profiles with peak frequencies as high as 32 c/deg. Marr *et al.*, (1980) estimated the smallest possible channel of human vision on the basis of retinal properties. They estimated the excitatory center to be about 0.022° in diameter, i.e. about three cones. If we assume the center frequency of this channel to correspond to a 6 cone period, this is 21 c/deg. De Valois *et al.*, (1982) reported finding no striate cortical cells in the macaque with center frequencies higher than 16 c/deg. Perhaps, as the width of the 32 c/deg grating is decreased, we rely increasingly on the spatial frequency channels tuned to frequencies farther away, but never activate a phase coherent filter centered at 32 c/deg. In support of this, the psychometric functions for gratings of 32 c/deg with a width

of one cycle in noise have slopes significantly greater than 1, as shown in Table 2.

Thresholds in the absence of noise

Why does spatial summation in the absence of visual noise extend over more cycles? Watson *et al.*, (1983) found maximum quantum efficiency for a drifting (4 Hz) 7 c/deg Gabor function about 3 cycles in width (0.52 octaves at half-height).

At threshold, phase information may not be fully available. The observer may not be able to monitor a phase coherent channel efficiently. As an alternative, he seeks to look at as many channels as possible, increasing the region of spatial summation (and narrowing the estimated bandwidth). Another consequence of this strategy is that the psychometric function might steepen both because of incoherent detection and because of channel uncertainty.

Legge and Foley (1980) have reported a dichotomy in the detection of sinusoidally masked high-contrast gratings versus low-contrast gratings. There seems to be less spatial pooling for high contrast grating discrimination than for the low contrast gratings. This is analogous to the results of this study. For low-contrast masking tuning function, Legge and Foley (1980) find narrower bandwidths, about 0.5 octaves. Low-contrast psychophysical techniques tend to estimate narrower bandwidths (e.g. Sachs, Nachmias and Robson, 1971). [However, Arend and Lange (1980) have calculated narrower bandwidths from contrast matching studies.] Perhaps in accord with this is the present observation that contrast-energy thresholds for gratings in the absence of noise rise very little over a region which includes more than one cycle, suggesting effectively narrower bandwidths. However, efficiencies change too slowly to be attributed to a single cross-correlator.

SUMMARY

For detection of stationary gratings in dynamic noise, efficiency was highest for a grating about one cycle wide. The profile (luminance vs width in cycles) of this "best seen" pattern is shown in Fig. 5. Efficiency as a function of width declined on either side of one cycle in a manner consistent with cross-correlation with the pattern shown in Fig. 5. The slope of the psychometric function was consistent with the cross-correlation hypothesis. Efficiency for patterns in the absence of noise declined much more slowly as the width of the pattern was extended beyond one cycle.

Acknowledgements—I would like to thank Dr G. E. Legge, Dr D. Pelli, Dr G. Rubin and G. Wakefield for many hours of useful discussion. I also wish to thank Drs H. B. Barlow, N. Viemeister, D. Burkhardt, R. Purple and H. Gershenson, for criticisms and suggestions. M. Bergman, B. Witkofsky, M. Schleske and D. Koenen provided technical support. Joanne Kersten typed. The experiments reported in this paper formed part of a doctoral dissertation submitted to the University of Minnesota. The research was supported by PHS grant EY02857 to Dr Legge and a University of Minnesota Doctoral Dissertation Grant. This paper was completed at the Physiological Laboratory, University of Cambridge, with the support of an NIH postdoctoral fellowship EY05660.

REFERENCES

Arend L. E. and Lange R. V. (1980) Narrow-band spatial mechanisms in apparent contrast matching. *Vision Res.* **20,** 143–148.

Barlow H. B. (1958) Temporal and spatial summation in human vision at different background intensities. *J. Physiol.* **141,** 337–350.

Barlow H. B. (1962) A method of determining the overall quantum efficiency of visual discriminations. *J. Physiol.* **160,** 155–168.

Barlow H. B. (1978) The efficiency of detecting changes of density in random dot patterns. *Vision Res.* **18,** 637–650.

Blackwell H. (1946) Contrast thresholds of the human eye. *J. opt. Soc. Am.* **36,** 624–643.

Blakemore C. and Campbell F. W. (1969) On the existence of neurones in the human visual system selectively sensitive to the orientation and size of retinal images. *J. Physiol.* **203,** 237–260.

Burgess A. E., Wagner R. F., Jennings R. J. and Barlow H. B. (1981) Efficiency of human visual signal discrimination. *Science* **214,** 93–94.

Campbell F. W. and Green D. G. (1965) Optical and retinal factors affecting visual resolution. *J. Physiol.* **181,** 576–596.

De Valois R. L., Albrecht D. G. and Thorell L. G. (1982) Spatial frequency selectivity of cells in macaque visual cortex. *Vision Res.* **22,** 545–559.

De Vries H. (1943) The quantum character of light and its bearing upon the threshold of vision, the differential sensitivity and acuity of the eye. *Physica,* **10,** 553–564.

Esteves O. and Cavonius C. R. (1976) Low-frequency attenuation in the detection of gratings: Sorting out the artifacts. *Vision Res.* **16,** 497–500.

Gabor D. (1946) Theory of communication. *J. I.E.E.E., Lond.* **93,** 429–457.

Graham C. H., Brown R. H. and Mote F. A. (1939) The relation of size of stimulus and intensity in the human eye. I. Intensity thresholds for white light. *J. exp. Psychol.* **24,** 555–573.

Graham N. and Nachmias J. (1971) Detection of grating patterns containing two spatial frequencies: A comparison of single-channel and multiple-channel models. *Vision Res.* **11,** 251–259.

Green D. M. and Swets J. A. (1974) *Signal Detection Theory and Psychophysics.* Wiley, New York.

Hecht S., Shlaer S. and Pirenne M. H. (1942) Energy, quanta, and vision. *J. gen. Physiol.* **25,** 819–840.

Hinkley D. V. (1969) Inference about the intersection in two phase regression. *Biometrika* **56,** 495–504.

Hinkley D. V. (1971) Inference in two-phase regression. *J. Am. Stat. Assoc.* **66,** 736–743.

Hoekstra J., van der Groot D. P. J., van den Brink G. and Bilsen F. A. (1974) The influence of the number of cycles upon the visual contrast threshold for spatial sine-wave patterns. *Vision Res.* **14,** 365–368.

Horowitz P. and Hill W. (1980) *The Art of Electronics.* Cambridge Univ Press.

Howell E. R. and Hess R. F. (1978) The functional area for summation to threshold for sinusoidal gratings. *Vision Res.* **18,** 369–374.

Jones R. C. (1959) Quantum efficiency of human vision. *J. opt. Soc. Am.* **49,** 645–653.

Legge G. E. (1978) Space domain properties of a spatial frequency channel in hu
959–969.

Legge G. E. and Foley J. M
human vision. *J. opt. Soc*

Maffei L., Morrone C., Pirc
Responses of visual corti
periodic stimuli. *J. Physic*

Marcelja S. (1980) Math
responses of simple corti
1297–1300.

Marr D. (1982) *Vision.* Free

Marr D., Poggio T. and Hild
in early human vision. *J.*

Movshon J. A., Thompson
Spatial summation in the r
the cat's striate cortex. *J.*

Nolte L. W. and Jaarsma D
of one of M. orthogonal
497–505.

Peichl L. and Wassle H. (197
ganglion cell receptive fie
Physiol. **291,** 117–141.

Pelli D. (1981) Effects of V
bridge Univ., England.

Pelli D. (1984) Intrinsic unc
of visual detection. *J. opt*

Pentland A. P. (1982) Percep
opt. Soc. Am. **72,** 1756.

Roberts T. A. (1963) Analy
non-linear shift register g
Conf., pp. 390–399. IEE,

Robson J. G. and Graham N
and regional variation in
visual field. *Vision Res.* **2**

Rose A. (1948) The sensiti
absolute scale. *J. opt. Soc*

Rubin G. S. (1982) Suppress
lar pattern vision. Ph.D.
ogy, University of Minne

Sachs M. B., Nachmias J. an
frequency channels in hum
1176–1186.

Sakitt B. and Barlow H.
economical encoding of
cortex. *Biol. Cybernet* **43,**

Savoy R. L. and McCann
spatial-frequency sine-wav
ber of cycles. *J.opt. Soc.*

Stiles W. S. and Crawford B
ness increment for white l
the foveal and parafovea
55–102.

Stromeyer C. F. and Jules
masking in vision: Critical
J. opt. Soc. Am. **62,** 1221

Tanner W. P. and Birdsall T
η as psychophysical mea
922–928.

Tolhurst D. J., Movshon J.
statistical reliability of sig
monkey visual cortex. *Vi*

Tolhurst D. J. and Thomps
of spatial frequency selecti
17 of the cat. *Proc. R. S*

Van Meeteren A. and Barlo
efficiency for detecting sin
dot density in random fig

Watson A. B. (1979) Prob
Vision Res. **19,** 515–522.

Watson A. B. (1982) Summ
cates many types of det
Vision Res. **22,** 17–25.

Watson A. B. and Pelli D.

frequency channel in human vision. *Vision Res.* **18,** 959–969.
Legge G. E. and Foley J. M. (1980) Contrast masking in human vision. *J. opt. Soc. Am.* **70,** 1458–1471.
Maffei L., Morrone C., Pirchio M. and Sandini G. (1979) Responses of visual cortical cells to periodic and non-periodic stimuli. *J. Physiol.* **296,** 27–47.
Marcelja S. (1980) Mathematical description of the responses of simple cortical cells. *J. opt. Soc. Am.* **70,** 1297–1300.
Marr D. (1982) *Vision.* Freeman, San Franscisco.
Marr D., Poggio T. and Hildreth E. (1980) Smallest channel in early human vision. *J. opt. Soc. Am.* **70,** 868–870.
Movshon J. A., Thompson I. D. and Tolhurst D. J. (1978) Spatial summation in the receptive fields of simple cells in the cat's striate cortex. *J. Physiol.* **283,** 53–77.
Nolte L. W. and Jaarsma D. (1967) More on the detection of one of M. orthogonal signals. *J. acoust. Soc. Am.* **41,** 497–505.
Peichl L. and Wassle H. (1979) Size, scatter and coverage of ganglion cell receptive field centres in the cat retina. *J. Physiol.* **291,** 117–141.
Pelli D. (1981) Effects of Visual Noise. Ph.D thesis Cambridge Univ., England.
Pelli D. (1984) Intrinsic uncertainty explains many aspects of visual detection. *J. opt. Soc. Am.* In press.
Pentland A. P. (1982) Perception of shape from shading. *J. opt. Soc. Am.* **72,** 1756.
Roberts T. A. (1963) Analysis and synthesis of linear and non-linear shift register generators. *Inter. Telemetering Conf.*, pp. 390–399. IEE, Savoy Place, London.
Robson J. G. and Graham N. (1981) Probability summation and regional variation in contrast sensitivity across the visual field. *Vision Res.* **21,** 409–418.
Rose A. (1948) The sensitivity of the human eye on an absolute scale. *J. opt. Soc. Am.* **38,** 196–208.
Rubin G. S. (1982) Suppression and summation in binocular pattern vision. Ph.D. thesis, Department of Psychology, University of Minnesota.
Sachs M. B., Nachmias J. and Robson J. G. (1971) Spatial-frequency channels in human vision. *J. opt. Soc. Am.* **61,** 1176–1186.
Sakitt B. and Barlow H. B. (1982) A model for the economical encoding of the visual image in cerebral cortex. *Biol. Cybernet* **43,** 97–108.
Savoy R. L. and McCann J. J. (1975) Visibility of low-spatial-frequency sine-wave targets: Dependence on number of cycles. *J.opt. Soc. Am.* **65,** 343–350.
Stiles W. S. and Crawford B. H. (1934) The liminal brightness increment for white light for different conditions of the foveal and parafoveal retina. *Proc. R. Soc. B* **116,** 55–102.
Stromeyer C. F. and Julesz B. (1972) Spatial-frequency masking in vision: Critical bands and spread of masking. *J. opt. Soc. Am.* **62,** 1221–1232.
Tanner W. P. and Birdsall T. G. (1958) Definitions of d′ and η as psychophysical measures. *J. acoust. Soc. Am.* **30,** 922–928.
Tolhurst D. J., Movshon J. A. and Dean A. F. (1983) The statistical reliability of signals in single neurons in cat and monkey visual cortex. *Vision. Res.* **23,** 775–785.
Tolhurst D. J. and Thompson I. D. (1981) On the variety of spatial frequency selectivities shown by neurons in area 17 of the cat. *Proc. R. Soc. Lond B* **213,** 183–199.
Van Meeteren A. and Barlow H. B. (1981) The statistical efficiency for detecting sinusoidal modulation of average dot density in random figures. *Vision Res.* **21,** 765–789.
Watson A. B. (1979) Probability summation over time. *Vision Res.* **19,** 515–522.
Watson A. B. (1982) Summation of grating patches indicates many types of detector at one retinal location. *Vision Res.* **22,** 17–25.
Watson A. B. and Pelli D. G. (1983) QUEST: A Bayesian adaptive psychometric method. *Percept. Psychophys.* **33,** 113–120.
Watson A. B., Barlow H. B. and Robson J. G. (1983) What does the eye see best? *Nature* **302,** 419–422.
Wilson H. R. and Bergen J. R. (1979) A four mechanism model for threshold spatial vision. *Vision Res.* **19,** 19–32.
Wright M. J. (1982) Contrast sensitivity and adaptation as a function of grating length. *Vision Res.* **22,** 139–149.

APPENDIX 1

Contrast energy of a Gabor Function

The contrast function of a cosine Gabor function is

$$c(x) = c_m \exp(-x^2/s_x^2)\cos(2\pi f x).$$

$$s^2 = \int c^2(x)\mathrm{d}x = \int c_m^2 \exp(-2x^2/s_x^2)\cos^2(2\pi f x)\mathrm{d}x$$

where the integration limits are $\pm\infty$. Using the identity

$$2\cos^2 t \equiv \cos 2t + 1$$

we have

$$s^2 = 0.5c_m^2 \int \exp(-2x^2/s_x^2)\{\cos 4\pi f x) + 1\}\mathrm{d}x.$$

This can be evaluated using the standard definite integral

$$\int \exp(-x^2/s_x^2)\cos(bx)\mathrm{d}x = \sqrt{\pi} s_x \exp(-b^2 s_x^2/4).$$

Thus we have

$$s^2 = 0.5c_m^2 s_x \sqrt{(\pi/2)}\{1 + \exp(-2\pi^2 f^2 s_x^2)\}.$$

Including time (t), the contrast energy is

$$s^2 = 0.5^2 c_m{}^2 s_x \sqrt{(\pi/2)} s_t \sqrt{(\pi/2)}\{1 + \exp(-2\pi^2 f^2 s_x^2)\}\{2\}$$

for a time constant s_t.

APPENDIX 2

Efficiency of a "mis-matched" cross-correlator

Let $s(x)$ and $f(x)$ be the signal and filter functions represented by

$$s(x) = c_m \exp\{-(x/s_1)^2\}\cos(2\pi f_1 x + \phi)$$
$$f(x) = \exp\{-(x/s_0)^2\}\cos(2\pi f_0 x)$$

where s_1 and s_0 are the space constants for the signal and filter. ϕ is the relative phase. The frequencies are f_1 and f_0 for the signal and filter respectively. Then the output of the cross-correlator is given by

$$r_0 = \int f(x)s(x)\mathrm{d}x$$
$$= \int c_m \exp\{-(x/s_1)^2\}\cos(2\pi f_1 x + \phi) \times \exp\{-(x/s_0)^2\}\cos(2\pi f_0 x)\mathrm{d}x.$$

Using the fact that

$$\cos(2\pi f_1 x + \phi) = \cos(2\pi f_1 x)\cos\phi - \sin(2\pi f_1 x)\sin\phi,$$

and the identity

$$\cos\alpha\cos\beta \equiv 0.5\{\cos(\alpha+\beta) + \cos(\alpha-\beta)\}$$

we have

$$r_0 = 0.5\int \exp\{-x^2(1/s_1^2 + 1/s_0^2)\}\{\cos[2\pi(f_1+f_0)x] \cos[2\pi(f_1-f_0)\times]\}\cos\phi\,\mathrm{d}x$$

where the integral with the odd-symmetric integrand has been dropped. Let

$$1/s'^2 = 1/s_1^2 + 1/s_0^2$$

and

$$f_a = f_1 + f_0,\ f_b = f_1 - f_0.$$

Integrating the expression for r_0, we have

$$r_0 = c_m\sqrt{\pi}s'[\exp\{-(\pi f_a s')^2\} + \exp\{-(\pi f_b s')^2\}]\cos\phi.$$

Efficiency (E) is inversely proportional to contrast-energy threshold (s^2)

$$E \propto 1/s^2 \propto 1/\{c_m^2 s_1[\exp(-2\pi^2 f_1^2 s_1^2) + 1]\}$$

(see Appendix 1). For the case of this paper

$$f_1 = f_0, \phi = 0.$$

Thus, the contrast threshold is proportional to

$$c_m \propto 1/\{\sqrt{\pi}s'[1 + \exp(-4\pi^2 f_1^2 s'^2)]\}.$$

By inserting this value of c_m into the above expression for efficiency, the efficiency is determined to within a multiplicative constant. The efficiency is 1 when $s_1 = s_0$.

Vision Res. Vol. 24, No. 12, pp
Printed in Great Britain. All ri

A METH

Clinical Neurophys

Abstract—A metho
geometry of distorti
and radial distortio
Image luminance d
A unidirectional gra
central value over t
orientations distorti
applications in visi
surface has been ge
is described to dem

Human vision Fi

Visual experiments usual
ditions by using limite
experiments the stimulus
diameter and thus occup
angle of the monocular vi
than half of its estima
(Drasdo, 1977). The maj
visual field then has diffe
for spatial and temporal
nance and spectral con
Inevitably therefore the
leading results when rela
iour. To add to these di
detects low spatial frequ
eral interaction propertie
fore affected by the ec
stimulus. This has been re
example in the case of
contrast sensitivity (Scho
der Wildt and Waarts,
limited fields can seriously

Surprisingly it has beer
images occupying the tot
distortion. This avoids th
field. The technique is si
applications.

THEORY A

When an image is proje
which has the form of a su
axis passes through the pr